Available online at www.sciencedirect.com
SCIENCE DIRECT
Catalysis Today 99 (2005) 347–357
CATALYSIS TODAY
www.elsevier.com/locate/cattod

Nano-structured CeO_2 supported Cu-Pd bimetallic catalysts for the oxygen-assisted water–gas-shift reaction

Elise S. Bickford, Subramani Velu, Chunshan Song*

Clean Fuels and Catalysis Program, The Energy Institute and Department of Energy and Geo-Environmental Engineering, The Pennsylvania State University, 209 Academic Projects Building, University Park, PA 16802, USA

Available online 15 December 2004

Abstract

The present work focuses on the development of novel Cu-Pd bimetallic catalysts supported on nano-sized high-surface-area CeO_2 for the oxygen-assisted water–gas-shift (OWGS) reaction. High-surface-area CeO_2 was synthesized by urea gelation (UG) and template-assisted (TA) methods. The UG method offered CeO_2 with a BET surface area of about 215 m^2/g, significantly higher than that of commercially available CeO_2. Cu and Pd were supported on CeO_2 synthesized by the UG and TA methods and their catalytic performance in the OWGS reaction was investigated systematically. Catalysts with about 30 wt% Cu and 1 wt% Pd were found to exhibit a maximum CO conversion close to 100%. The effect of metal loading method and the influence of CeO_2 support on the catalytic performance were also investigated. The results indicated that Cu and Pd loaded by incipient wetness impregnation (IWI) exhibited better performance than that prepared by deposition–precipitation (DP) method. The difference in the catalytic activity was related to the lower Cu surface concentration, better Cu–Ce and Pd–Ce interactions and improved reducibility of Cu and Pd in the IWI catalyst as determined by the X-ray photoelectron spectroscopy (XPS) and temperature-programmed reduction (TPR) studies. A direct relation between BET surface area of the CeO_2 support and CO conversion was also observed. The Cu-Pd bimetallic catalysts supported on high-surface-area CeO_2 synthesized by UG method exhibited at least two-fold higher CO conversion than the commercial CeO_2 or that obtained by TA method. The catalyst retains about 100% CO conversion even under extremely high H_2 concentration.

Keywords: Catalyst; Oxygen-assisted water–gas-shift; H_2 production; CeO_2; Cu–Pd; Bimetallic catalysts; Fuel processor

1. Introduction

Fuel cell technology is rapidly on the rise. With an increased demand for fuel and energy efficiency over the modern combustion engine, fuel cells are a viable alternative. There is also added benefit of being more environment friendly by reducing emissions of pollutants and greenhouse gas. With the introduction of proton exchange membrane fuel cells (PEMFCs) for the use in automotive technology, it has become increasingly important to decrease the CO concentration of the feed gas to less than 10 ppm. Unlike solid oxide fuel cells and molten carbonate fuels cells wherein carbon monoxide can be used as a fuel, in the PEMFC, CO causes detrimental effects on the anode catalyst of the fuel cell. As the CO concentration increases, so do the voltage losses in the fuel cell [1] even at values as low as 10–100 ppm. The presence of CO in the feed gas causes irreversible poisoning of the catalyst in the electrodes [2], which will not only contribute to cell voltage losses, but also limit the life of the fuel cell.

In order to reduce the CO content in the feed gas obtained from fuel reforming to a tolerable level (less than 10 ppm), it is necessary to find a more active and more effective catalyst [3]. Two reactions that contribute to CO clean-up and need improved catalysts are the water–gas-shift (WGS) and preferential oxidation (PrOx) reactions. These reactions are represented in Eqs. (1) and (2), respectively, while the oxygen-assisted WGS reaction (OWGS) involves these two reactions, listed in Eq. (3), where the oxygen is incorporated

* Corresponding author. Tel: +1 814 863 4466; fax: +1 814 865 3248.
E-mail address: csong@psu.edu (C. Song).

0920-5861/$ – see front matter © 2004 Elsevier B.V. All rights reserved.
doi:10.1016/j.cattod.2004.10.010

in our design concept to facilitate the WGS reaction over new catalysts to reach low CO outlet concentration.

$$CO + H_2O \rightarrow CO_2 + H_2 \quad (1)$$

$\Delta H^\circ = 41.1$ kJ/mol; $\Delta G^\circ = -28.6$ kJ/mol

$$CO + \frac{1}{2}O_2 \rightarrow CO_2 \quad (2)$$

$\Delta H^\circ = -241.1$ kJ/mol; $\Delta G^\circ = -228.6$ kJ/mol

$$(1+x)CO + H_2O + \frac{x}{2}O_2 \rightarrow (1+x)CO_2 + H_2 \quad (3)$$

The water–gas-shift reactor, which significantly reduces the CO concentration down stream of the reformer, is the critical component of the fuel processor. $Cu/ZnO/Al_2O_3$ commercial catalysts have long been used in the water–gas-shift reaction [4–6]. Although the results have been positive, it is very difficult to achieve CO levels below 10 ppm with these catalysts. In addition, the catalysts are pyrophoric and consequently, they degrade during operation, particularly when exposed to air. The water–gas-shift reactor is often the largest component of the fuel processor and its performance is based on the activity of the catalyst.

The commonly used $Cu/ZnO/Al_2O_3$ catalyst has been extensively studied in this area and there is a vast amount of research to understand the behavior of this type of catalyst from kinetic modeling [7] to calcination temperature studies [8]. Hadden et al. [9] have shown that the activity of the $Cu/ZnO/Al_2O_3$ can be correlated to the Cu surface area under controlled precipitation and aging conditions from 38 to 61 wt% Cu. This conclusion is later reinforced by Utaka et al. [5].

Utaka et al. [5] have demonstrated that the activity of the catalyst depends largely on the surface area and crystallinity. They also stated that the CO removal is largely dependant on the space velocity and that the thermodynamic equilibrium is achieved at a low space velocity. This demonstrates the need for highly active catalysts and they were able to obtain 90% CO conversion at 150 °C with an addition of 2% O_2 to the feed steam with catalysts calcined at 500 or 700 °C.

Sohrabi and Irandoukht [8] have studied the effect of calcination temperature on the reaction behavior. They have found that the total surface area decreases with increase in the calcination temperature of the catalyst. This decrease in surface area is expected to further decrease the activity of the catalyst by reducing the number of active sites on the surface. The authors have found that the particle size on the support surface gradually increased from 300 to 500 °C, but increased sharply from 500 to 700 °C, thereby suggesting that the calcination temperature of the catalyst should be kept below 500 °C for optimum performance.

Prakash [10] studied the effect of syngas composition ($CO + H_2$) on the water–gas-shift reaction. It was found that the optimum H_2O concentration decreased with an increase in the temperature of reactor. The author has also found that the water concentration increased as the H_2/CO ratio decreased in a model system.

In an early study by Sekizawa et al. [11] on the catalytic activity of Cu on alumina-mixed oxides supports, it was found that Cu (30)/Al_2O_3–ZnO had the highest activity for the water–gas-shift reaction. They have also found that if half the stoichiometric amount of oxygen/carbon monoxide was added to the gas feed, the CO removal in the system was greatly enhanced.

This led to later work by the same group [5] further investigating the phenomenon. It was found that the activity of the catalyst depended on surface area and crystallinity, but that CO removal also was largely dependant on the space velocity of the reaction. They suggested that since thermodynamic equilibrium is achieved at low space velocities, a highly active catalyst is needed.

While investigating Ru-based catalysts for the selective oxidation of CO using the oxygen-assisted water–gas-shift reaction, Worner et al. [12] found that using 8% Ru on a Al_2O_3 wash-coat over SiC foamed ceramic, less than 30 ppm of CO could be achieved. The feed gas was based on 4000 ppm CO, 6000 ppm O_2, and 4% H_2O at low temperature and VHSV of 5000 h^{-1}. These results and the results achieved for the individual water–gas-shift and preferential oxidation reactions are encouraging for the direction of this work on the addition of oxygen to the water–gas-shift feed stream.

The objective of the present investigation was to develop a new CeO_2-based Cu-Pd bimetallic catalyst for low-temperature oxygen-assisted WGS reaction for on-board or on-site fuel cell applications in order to reduce the CO concentration in the outlet of methanol reformer in a single reactor to below 10–30 ppm suitable for PEM fuel cells.

2. Experimental

2.1. Synthesis of CeO_2 support

2.1.1. Urea gelation

The urea gelation (UG) method for support preparation is similar to that used by Kundakovic and Flytzani-Stephanopoulos [13]. An appropriate molar amount of metal salt [$(NH_4)_2Ce(NO_3)_6$ and $ZrO(NO_3)_2{\cdot}H_2O$] was placed in a beaker and 300 mL of deionized H_2O was added. As an example, for 50% CeO_2–50% ZrO_2, 30 g of $(NH_4)_2Ce(NO_3)_6$ and 24.4 g of $ZrO(NO_3)_2{\cdot}H_2O$ were used. The mixture was stirred and heated until the salts were dissolved. Forty-five grams of urea (H_2NCONH_2) was dissolved in 100 mL of deionized H_2O. The urea was then added to the metal salt solution. The solution was heated at ~120 °C and allowed to boil until precipitation occurred. Once precipitation began, the suspension was boiled for another 3.5 h to remove NH_3 and age the support. The filtered support was dried in an oven overnight and then calcined at 2 °C/min to 450 °C and held for 3–4 h in a furnace. A temperature of 450 °C was chosen as the optimum calcination temperature for CeO_2 from data in Zhang et al. [14].

2.1.2. Template-assisted synthesis

The template-assisted (TA) method used for the support preparation was modified from previous work done by Lyons et al. [15]. An appropriate amount of *n*-hexadecylamine was added to 100 mL of 1:1 volume ratio of H_2O:ethanol. The metal salt precursors [$(NH_4)_2Ce(NO_3)_6$ and $ZrO(NO_3)_2 \cdot H_2O$] were added in proper ratios into the solution at a 1:1 molar ratio of metal salt:surfactant. As an example, for the preparation of 50% CeO_2–50% ZrO_2, 30 g of $(NH_4)_2Ce(NO_3)_6$ and 24.4 g of $ZrO(NO_3)_2 \cdot H_2O$ and 6.6 g of *n*-hexadecylamine were used. Solutions were then stirred for 1 h at room temperature for aging. The solutions were then placed in an oven at 120 °C for one day. The dried fraction was then removed and washed with a H_2O:ethanol solution and then liberally washed with water by Buchner filtration. The support was then dried in an oven overnight and calcined at 2 °C/min to 450 °C and held for 3–4 h in a furnace.

2.2. Metal impregnation

2.2.1. Incipient wet impregnation

For incipient wet impregnation (IWI), a minimum amount of solvent should be added to the support. The catalyst support saturation limit (incipient wetness volume) was first determined by adding solvent drop by drop; for CeO_2, it was determined to be 0.5 mL/g. The metal salts, $Cu(NO_3)_2 \cdot 5H_2O$ and $Pd(CH_3COO)_2$ or $H_2PtCl_6 \cdot xH_2O$, were dissolved in a minimal amount of deionized H_2O or acetone. The salt solutions were added to the support drop-wise. After all of the solutions were added, a small amount of appropriate solvent was used to wash the beaker and remove remaining salt. The impregnated supports were then placed in an oven at 120 °C and dried overnight. After drying, the catalysts were calcined to 400 °C, at a heating rate of 2 °C/min, and held for 3–4 h.

2.2.2. Deposition–precipitation

The deposition–precipitation (DP) method used for catalyst preparation is described in the literature [16]. CeO_2/ZrO_2 was placed in a beaker and submerged in H_2O. Appropriate solutions of $Cu(NO_3)_2 \cdot 5H_2O$ in H_2O and $Pd(CH_3COO)_2$ in acetone were prepared. Meanwhile, the pH of the CeO_2/H_2O suspension was adjusted to ~9.2 using dilute KOH solution and then the salt solution was added drop-wise to the CeO_2/H_2O slurry. $Cu(NO_3)_2 \cdot 5H_2O$ aqueous solution was added first, followed by a $Pd(CH_3COO)_2$ acetone solution. Due to the high metal content, it was necessary to impregnate the support to the saturation limit, let dry in an oven at 110 °C, and then impregnate the remaining metal solution. After complete addition, the pH of the solution was measured and adjusted to ~9.0. The solution was aged for 1 h at room temperature and filtered and washed with distilled water until the pH of the filtrate was 7. The catalysts were dried overnight at 120 °C before calcination to 400 °C, with a heating rate of 2 °C/min, and held at 400 °C for 3–4 h.

2.3. Catalysts characterization

The structural properties of catalysts were investigated by powder X-ray diffraction (XRD) and N_2 adsorption–desorption experiments. XRD data were collected on a Scintag instrument. Data acquisition took place in the continuous mode, with a 4° step in the 2Θ range 5–70°. The sample was ground to a fine powder and mounted on a zero-background quartz slide. The particle sizes of the CeO_2 samples were calculated by X-ray line broadening technique using Debye–Scherer equation, $t = 0.9\lambda/\beta \cos \Theta$, where t is the particle size, λ the wavelength of radiation used (1.541 Å), β the line broadening of the peak or full-width at half maximum (FWHM; rad), and Θ is the angle of the diffraction peak. The BET surface areas of CeO_2 supports as well as supported catalysts were determined by N_2 adsorption–desorption isotherms at 77.3 K, on a Micromeritics ASAP 2000 instrument. The bulk compositions of the catalyst were analyzed by inductively coupled plasma-mass spectrometry (ICP-MS) using a Finnigan MAT ELEMENT high-resolution ICP-MS with Merchantek Nd-YAG laser for direct solids analysis.

The surface properties of the catalysts were evaluated by X-ray photoelectron spectroscopy (XPS) using Kratos Analytical Axis Ultra, with a monochromatic aluminum X-ray source of 1486.6 eV. An X-ray power of 280 W was used with charge neutralization of low energy electrons. A take-off angle of 90° was used on a spot size of 700 μm × 350 μm. The charge was corrected with respect to C 1s spectrum at 285.00 eV. The samples were mounted on a double-sided adhesive tape and had an approximate sample depth of 25 Å. Quantification was performed by applying appropriate sensitivity factors for the Kratos instrument. The sensitivity factors help account for X-ray cross-section and the transmission function of the spectrometer. All XPS analysis was performed at the Materials Characterization Lab at Penn State University by laboratory staff.

The redox properties of the catalysts were investigated by temperature-programmed reduction (TPR) on Micromeritics AutoChem 2910 TPR/TPD Analyzer. About 0.1 g of the sample was loaded in the reactor and heated at the rate of 10 °C/min in 5% H_2–Ar gas mixture flowing at the rate of 25 mL/min. The H_2 consumption due to sample reduction was simultaneously monitored by TCD detector, and the data were processed by GRAMS 32 software.

The surface morphology of a few selected samples was analyzed using a Hitachi S-3500N scanning electron microscope (SEM). The accelerating voltage was set at 10 keV and secondary and back-scattered electrons were used. The catalyst samples were mounted by creating a slurry with ethanol and placed drop-wise on carbon tape on an aluminum SEM stub. The ethanol was then evaporated under vacuum before the sample was loaded into the SEM chamber. Selected area energy-dispersive X-ray (EDX) spectra were taken on the same sample stubs in the SEM chamber.

2.4. Catalytic studies

The WGS and oxygen-assisted WGS reactions were performed at 210 °C in a down-flow fixed-bed stainless steel reactor using 0.5 mL of the catalyst. Unless otherwise mentioned, the experimental conditions consisted of using an initial CO concentration of 2000 ppmv, and a gas hourly space velocity (GHSV) of 17,760 h^{-1}. The gas compositions used in the WGS reaction over the catalysts were 0.2% CO, 10% CO_2, 40.0% H_2O, and the balance was Ar gas. In the oxygen-assisted WGS reaction, 1.0% O_2 in the form of air was also added to the feed. The effluent of the reactor was analyzed on-line using an Agilent 3000 A Micro GC equipped with thermal conductivity detectors. The CO detection limit was well below 10 ppm. Prior to the reaction, the catalyst was reduced in situ at 250 °C for 2 h in H_2 gas (flow rate 15 cc/min).

3. Results and discussion

3.1. Physicochemical properties of various CeO_2 supports

The structural and textural properties of CeO_2 synthesized by the urea gelation and template-assisted methods have been evaluated by powder X-ray diffraction and N_2 adsorption–desorption measurements, and the results are compared with that of commercial CeO_2 obtained from Rhodia company. The XRD patterns shown in Fig. 1 for CeO_2 synthesized by UG (CeO_2-UG) and TA (CeO_2-TA) methods are very similar to those of the commercial CeO_2 (CeO_2-Comm.), demonstrating that the UG and TA methods employed in the present study produced pure CeO_2 phase. In fact, the XRD peak intensities of CeO_2-UG is very similar to that of CeO_2-Comm. while the CeO_2-TA exhibits larger intensities, indicating that the TA method produces more crystalline CeO_2. However, the BET specific surface area of CeO_2-TA is significantly less (104 m^2/g) compared to CeO_2-UG (215 m^2/g) and CeO_2-Comm. (154 m^2/g; see Table 1). It is interesting to note that high-surface-area CeO_2 having a BET surface area about 215 m^2/g has been synthesized in the present study and this is considerably higher than that of commercial CeO_2 (154 m^2/g). Recently, Flytzani-Stephanopoulos and co-workers synthesized nano-sized CeO_2 and 10% La doped CeO_2 by urea gelation method with BET surface areas in the range 90–150 m^2/g [17]. On the other hand, Velu et al. [18] have obtained CeO_2 with a BET surface area of 229 m^2/g using template-assisted method. The average pore diameter and mean pore volume of the CeO_2-UG synthesized in this study are also higher than those of CeO_2-Comm. The average particle sizes of CeO_2 samples determined by X-ray line broadening experiments (see Table 1) indicate that the samples are really nano-sized with particle sizes between 60 and 130 Å. Interestingly, the particle sizes of the sample synthesized by urea gelation method is even smaller (about 60 Å) than that of the commercial sample (about 70 Å). The sample synthesized by template-assisted method offered bigger particles of around 130 Å. These three types of CeO_2 samples have been used as supports for Cu and Pd in order to investigate the effect of the nature of CeO_2 support on the catalytic performance in the water–gas-shift and oxygen-assisted water–gas-shift reactions.

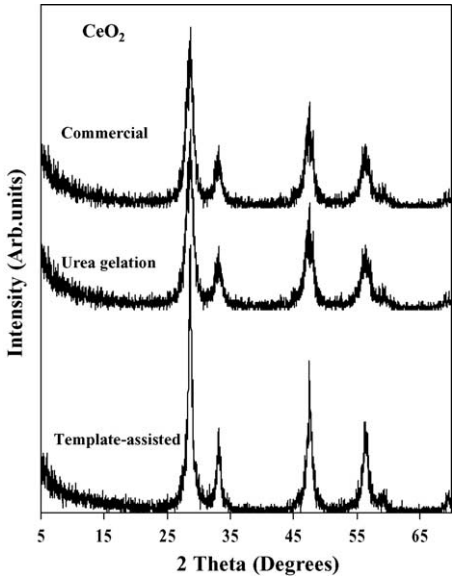

Fig. 1. Powder XRD patterns of CeO_2 supports obtained from commercial source, synthesized by urea gelation and template-assisted methods.

3.2. Optimization of Pd and Cu loadings

The commercial CeO_2 was used as a support for Pd and Cu to optimize the metal loadings as well as the experimental conditions such as temperature and space velocity. The Cu and Pd metals were loaded using the

Table 1
Textural properties of different CeO_2 supports

CeO_2 preparation method	BET surface area[a] (m^2/g)	Average pore diameter[a] (Å)	Mean pore volume[a] (cm^3/g)	Average particle sizes[b] (Å)
Commercial	154	33.2	0.14	70
Urea gelation	215	38	0.23	60
Template-assisted	104	42	0.12	130

[a] Determined by N_2 adsorption–desorption measurements.
[b] Calculated by X-ray line broadening method using Debye–Scherrer equation.

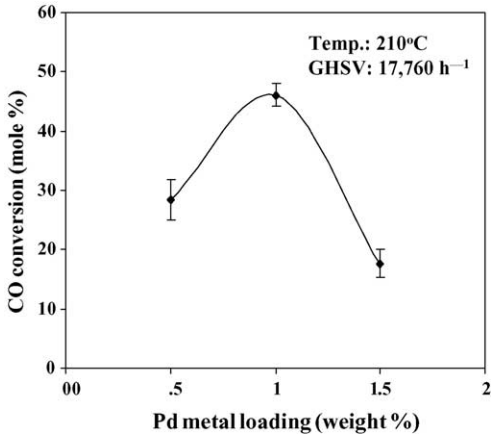

Fig. 2. Effect of Pd loading on the catalytic performance in WGS reaction over Cu-Pd/CeO_2 (comm.) catalyst containing 2 wt% Cu; catalytic activity after 4 h on-stream operation; feed compositions: 0.2% CO, 10% CO_2, 40.0% H_2O, and balance Ar.

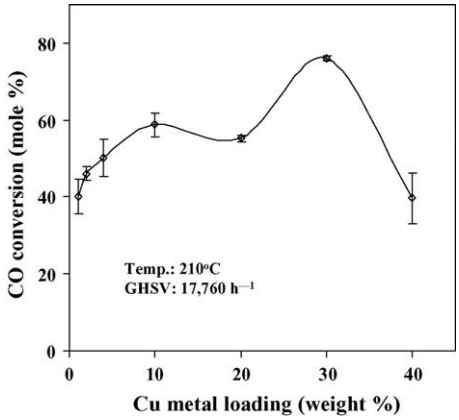

Fig. 3. Effect of Cu loading on the catalytic performance in WGS reaction over Cu-Pd/CeO_2 (comm.) catalyst containing 1 wt% Pd; catalytic activity after 4 h on-stream operation; feed compositions: 0.2% CO, 10% CO_2, 40.0% H_2O, and balance Ar.

deposition–precipitation method. The feed compositions used in the WGS reaction over the catalysts were 0.2% CO, 10% CO_2, 40% H_2O (steam), and the balance Ar. This feed composition was selected based on the CO concentration present in the reformed gas obtained from methanol reforming in our laboratory [19] and to further reduce the CO content to below 20 ppmw in the down stream for PEM fuel cell application.

Fig. 2 depicts the effect of Pd loadings on the catalytic performance in the WGS reaction for CO conversion at 210 °C at a gas hourly space velocity of 17,760 h^{-1}. The Cu content has been arbitrarily chosen to be 2 wt% by varying the Pd loading from 0.5 to 1.5 wt%. The results indicate that under the present experimental conditions, a maximum CO conversion of about 50 mole% could be achieved at 1 wt% Pd loading. A dramatic drop in CO conversion from about 50 mole% for 1 wt% Pd to below 20 mole% for 1.5 wt% Pd could be attributed to the excessive coverage of Cu surface by Pd. Since only about 50 mole% CO conversion could be achieved using the catalyst with 2 wt% Cu and 1 wt% Pd, the Cu content has been further increased by keeping the Pd loading at 1 wt%. The effect of Cu metal loading on the CO conversion under the same experimental conditions is shown in Fig. 3. It can be seen that a maximum CO conversion of about 80 mole% could be achieved at 30% Cu loadings. It should be noted that the CO conversion increases only by about 20 mole% (from about 40 to 60 mole%) by increasing the Cu loading from 2 to 10 wt%. The conversion remains unchanged around 55 mole% with increasing Cu content up to 20 wt%. However, the conversion increases sharply from about 55 to 80 mole% upon further increasing the Cu loadings from 20 to 30 wt% and then drops down to below 40 mole% when the Cu loading is increased beyond 40 wt%. The results therefore indicate that under the present experimental conditions, an optimum Cu loading of about 30 wt% is required to achieve a high CO conversion over the CeO_2 supported Cu-Pd bimetallic catalysts. This observation is in line with Sekizawa et al. [11] who also observed a maximum CO conversion at 30 wt% Cu loading in the Cu/ZnO-Al_2O_3 and Cu/CeO_2-Al_2O_3 catalysts. However, Li et al. [20] in their studies on the WGS reaction over CuCe(La) catalysts with Cu content from 5 to 40 wt% observed no significant change in the catalytic activity with increasing Cu content. Our results reveal that highly dispersed Cu clusters are responsible for better catalytic performance and sufficient number of Cu clusters would be formed on the CeO_2 surface at the Cu loadings of about 30 wt%. The BET surface area of La doped CeO_2 used by Li et al. [20] was less than two-thirds (91.7 m^2/g) of the BET surface area of CeO_2 used in the present study (BET surface area of commercial CeO_2 is 154 m^2/g). The higher surface area of CeO_2 used in the present study would require such a large Cu loading in order to form sufficient number of Cu clusters with optimum particle size.

3.3. Effect of space velocity

The effect of CO gas hourly space velocity on the catalytic performance has also been investigated using the Cu-Pd bimetallic catalyst with 30 wt% Cu and 1 wt% Pd supported on commercial CeO_2 [DP Cu (30)-Pd (1)/CeO_2 (comm.)] and the results are shown in Fig. 4. Under the given set of experimental conditions, and the addition of 1.6% air, the catalyst retains about 100% CO conversion until the GHSV of about 20,000 h^{-1} and then starts dropping slowly. Li et al. [20] observed about 50% drop in CO conversion when the GHSV was increased from 8000 to 80,000 h^{-1}. Andreeva et al. [21] have also noticed a significant drop in CO conversion with increasing GHSV from 4000 to 12,000 h^{-1} over Au/CeO_2 catalysts. Optimization of the catalyst formulations and their preparation methods in order to achieve a higher CO conversion close to 100% at higher GHSV is one of the prime objectives of the present study.

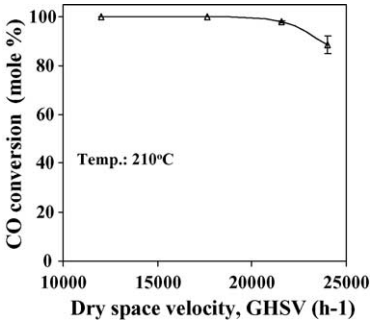

Fig. 4. Effect of gas hourly space velocity on the catalytic performance in the oxygen-assisted WGS reaction over DP Cu (30)-Pd (1)/CeO_2 (comm.) catalyst; catalytic activity after 4 h on-stream operation; feed compositions: 0.2% CO, 10% CO_2, 40.0% H_2O, 1% O_2 in air, and balance Ar.

3.4. Effect of method of metal loading

It is known that loading of precious metals by deposition–precipitation method offers a better metal dispersion and consequently a better catalytic performance in methanol synthesis, methanol decomposition, WGS, and hydrodechlorination reactions compared to the catalysts prepared by wet impregnation method [16,22–24]. In an effort to investigate if the DP method or the IWI method offers better CO conversion in the present study, the Cu-Pd bimetallic catalyst with 30 wt% Cu and 1 wt% Pd has also been prepared by IWI method and their catalytic performances are compared. It can be seen from Fig. 5 that the catalyst prepared by IWI method exhibits a CO conversion close to 100% compared to the catalyst prepared by DP method, which shows a slightly lower conversion of about 90 mole%. This observation is in contrast to the results reported in the references [16,22–24].

In order to understand the reason for the better activity of catalyst prepared by IWI compared to DP method, the physicochemical properties of these two catalysts have been

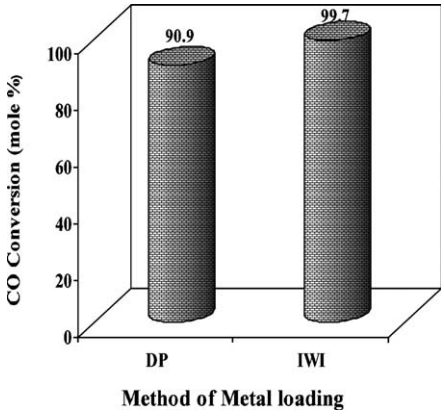

Fig. 5. Effect of method of Cu and Pd loading on the catalytic performance in the oxygen-assisted WGS reaction over Cu-Pd bimetallic catalysts containing 30 wt% Cu and 1 wt% Pd supported on the commercial CeO_2; feed compositions: 0.2% CO, 10% CO_2, 40.0% H_2O, 1% O_2 in air, and balance Ar.

Table 2
N_2 adsorption–desorption characteristics of various CeO_2-supported Cu-Pd bimetallic catalysts containing 30 wt% Cu and 1 wt% Pd

Catalyst	BET surface area (m^2/g)	Average pore diameter (Å)	Mean pore volume (cm^3/g)
DP Cu (30)-Pd (1)/CeO_2 (comm.)	85	35	0.09
IWI Cu (30)-Pd (1)/CeO_2 (comm.)	72	41	0.09
IWI Cu (30)-Pd (1)/CeO_2 (UG)	91	33	0.09
IWI Cu (30)-Pd (1)/CeO_2 (TA)	47	54	0.07

investigated by BET surface area measurements, X-ray photoelectron spectroscopy, and temperature-programmed reduction.

Table 2 compares the N_2 adsorption–desorption characteristics of catalysts prepared by DP and IWI methods. In both cases, the BET surface areas of metal loaded catalysts are about 80 m^2/g. The average pore diameter and the mean pore volume also are similar, indicating that there is no significant difference in the textural properties of these two catalysts.

The metal contents at the bulk and surface have been estimated using inductively coupled plasma-mass spectrometry technique and XPS, respectively, and the results are summarized in Table 3. It is interesting to note that although the bulk Cu, Pd, and Ce contents are similar between DP and IWI prepared catalysts, there is a significant difference in the surface compositions, particularly the Cu and Ce contents. The surface Cu content in the IWI catalyst is only half (14.5 wt%) that of DP catalyst (26.7 wt%). On the other hand, the surface Ce content is twice (9.5 wt%) in IWI catalyst compared to the DP catalyst (4.9 wt%). The surface Pd content is the same for both catalysts and it is about 0.4 wt% although the bulk Pd content is 1 wt%. It is likely that the lower Cu content and higher Ce content at the surface could be responsible for the overall better performance of the IWI catalyst (IWI Cu (30)-Pd (1)/CeO_2 (comm.)). The lower Cu content at the surface would favor a better dispersion of Cu metal on the CeO_2 support. On the other hand, the higher Cu content at the surface of DP catalyst could result in the lower Cu metal dispersion.

Table 3
Bulk and surface chemical compositions of Cu (30)-Pd (1)/CeO_2 (comm.) catalysts prepared by deposition–precipitation and incipient wetness impregnation methods

Catalyst	Bulk composition[a] (wt%)			Surface composition[b] (wt%)		
	Cu	Pd	Ce	Cu	Pd	Ce
DP Cu (30)-Pd (1)/CeO_2 (comm.)	35.1	1.0	49.1	26.7	0.4	4.9
IWI Cu (30)-Pd (1)/CeO_2 (comm.)	36.4	1.1	51.6	14.5	0.4	9.5

[a] Determined by ICP-MS.
[b] Determined by XPS.

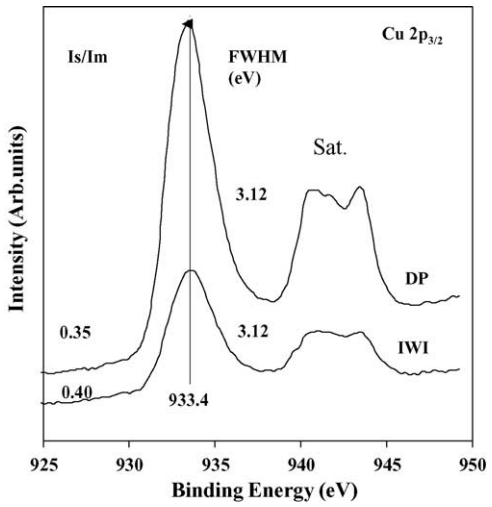

Fig. 6. Cu $2p_{3/2}$ XP spectra of DP Cu (30)-Pd (1)/CeO_2 (comm.) and IWI Cu (30)-Pd (1)/CeO_2 (comm.) catalysts.

Fig. 6 depicts the Cu $2p_{3/2}$ core level X-ray photoelectron spectra (XPS) of DP and IWI prepared catalysts. Both catalysts exhibit the Cu $2p_{3/2}$ main peak at 933.4 eV with a satellite peak at higher binding energy (BE) around 942 eV, characteristics of Cu^{2+} species. The peak intensity of DP catalyst is higher by over two-fold compared to that of IWI catalyst and this is clearly due to the lower Cu surface concentration of the later catalyst as evidenced from quantitative estimation (see Table 3). It should be recalled that the Cu surface concentrations of DP and IWI catalysts are 26.7 and 14.5 wt%, respectively, and this difference is clearly reflected in the intensity of XPS peaks. The full-width at half maximum of the main peak is the same for both catalysts and it is 3.12 eV. The intensity ratio between the satellite peak and the main peak (I_s/I_m) for DP catalyst is slightly lower (0.35) compared to that of IWI catalyst (0.4). The XPS spectrum of pure CuO exhibits the Cu $2p_{3/2}$ main peak at 933.8 eV with a FWHM of 3.6 eV and I_s/I_m ratio of 0.55 [25]. A comparison of Cu 2p BE, FWHM, and I_s/I_m of DP and IWI catalysts with those of CuO reveals that CuO-like species are present on the surface of CeO_2. However, the lower I_s/I_m ratio observed for DP and IWI catalysts compared to pure CuO suggests that at least, a part of Cu^{2+} ions are dissolved in the CeO_2 lattice to form a solid solution. The results also indicate the existence of a strong interaction between CuO and CeO_2. A similar decrease in I_s/I_m ratio has been observed in the CuZn-based methanol synthesis and reforming catalysts and the result has been attributed to the existence of a strong interaction between CuO and ZnO [25].

The existence of Cu–Ce interaction in the CuO/CeO_2 catalysts is well known in the literature [20,26–30]. A Cu–Ce redox equilibrium between Cu particles and CeO_2 support to stabilize the Cu^+ has been reported recently in the Cu/CeO_2 catalysts used in the methanol reforming reaction [26]. Liu and Flytzani-Stephanopoulos [28] have proposed a model for the stabilization of Cu^+ ions in the CeO_2 lattice and their transformation to the outer surface of copper oxide chain, $Cu^+{-}O{-}Cu{-}\cdots{-}O{-}Cu^+$. The authors have also confirmed the existence of Cu^+ species in their Cu/CeO_2 catalyst by using a combined XPS and Auger electron spectroscopy (AES). In XPS, the BE of Cu^+ (Cu_2O) has been observed around 932.4 eV [31]. Although the existence of Cu^+ species in the present catalyst system is not clearly discernable, the onset of the Cu $2p_{3/2}$ XP spectra around 930 eV and their asymmetric peak structure reveal that a mixture of Cu^{2+} and Cu^+ species could be present at the surface of the catalyst and they have a strong interaction with Ce species. The high surface concentration of Ce in the IWI catalyst compared to that of DP catalyst (see Table 3) would favor a strong Cu–Ce interaction at the surface to form relatively more Cu^+ species, and consequently a higher CO conversion (see Fig. 5). A combined XPS and AES study on both unreduced and reduced catalysts will be very useful to clearly understand the nature of Cu and Ce species present on the surface of these catalysts. Such studies are being conducted over these catalysts and the results will be reported in the near future.

The Pd 3d XP spectra of DP and IWI prepared catalysts are shown in Fig. 7. Unlike that observed in the Cu 2p spectra (Fig. 6), the intensity of Pd 3d spectra are similar for both catalysts and this is in accordance with the similar surface composition of about 0.4 wt% in both cases (see Table 3). The Pd $3d_{5/2}$ peak position for DP is lower by 0.6 eV (337.1 eV) compared to that of IWI catalyst, which appears at 337.7 eV. The Pd $3d_{5/2}$ BE of Pd metal, PdO, and $PdCl_2$ are reported to be 335, 336.3, and 337.8 eV, respectively [23,24]. The BE of the present catalysts is close to that of $PdCl_2$, indicating that the Pd is present in Pd^{2+} oxidation state. The higher BE of IWI catalyst compared to that of DP catalyst could be attributed to a strong interaction of Pd species with Ce surface. The strong interaction between Pd and Ce facilitates an easy electron

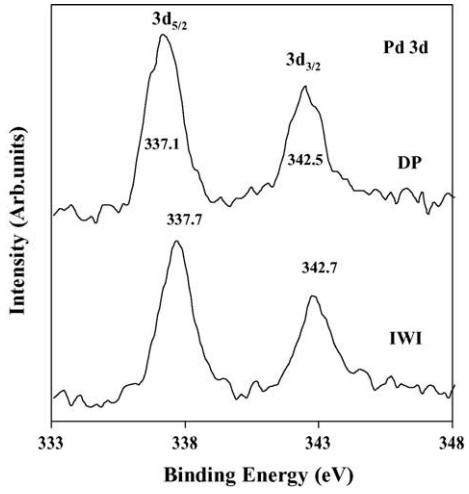

Fig. 7. Pd 3d XP spectra of DP Cu (30)-Pd (1)/CeO_2 (comm.) and IWI Cu (30)-Pd (1)/CeO_2 (comm.) catalysts.

transfer from Pd and Ce, making the Pd more electropositive and consequently higher BE. The formation of Pd cationic species in the reduced Pd/CeO_2 catalysts has been well documented in the literature [23,32,33]. The existence of such a strong interaction between Pd and Ce in the IWI catalyst could also contribute to the enhanced CO conversion observed in the present study.

In order to further investigate if the method of Cu and Pd loadings also affects the redox properties of the catalysts, which would also contribute to the difference in the observed catalytic activity, temperature-programmed reduction experiments have been performed using 5% H_2 in Ar as a reducing agent. The H_2-TPR has been extensively used in the literature to characterize the surface and bulk oxygen reducibility of doped and metal-loaded CeO_2 catalysts [20,24,26,30,34]. All the three components, namely CeO_2, PdO, and CuO, in the present catalyst system are reducible. In the case of CeO_2, the H_2-TPR shows two major reduction peaks, one around 500 °C for the reduction of surface capping oxygen and the other around 800 °C attributed to the reduction of bulk oxygen of CeO_2 [35]. Although the TPR experiments of the present study were performed up to 800 °C, for the sake of simplicity, the profiles in Fig. 8 are shown only up to 330 °C.

All the samples shown in Fig. 8 exhibit broad TPR profiles, indicating that reduction occurs in a wide temperature range between 120 and 240 °C and it is attributed to the reduction of PdO and CuO supported on CeO_2. The TPR profiles of 1% Pd/CeO_2 (UG), 30% Cu/CeO_2 (UG), and 30% Cu-1% Pd/CeO_2 (UG), all prepared by IWI method, have also been recorded under the similar experimental conditions (TPR profiles not shown). The 1% Pd/CeO_2 (UG) catalyst showed a single reduction peak centering at 153 °C. The 30% Cu/CeO_2 (UG) exhibited three distinct reduction peaks, centering at 159, 179, and 256 °C, respectively. On the other hand, the catalyst, 30% Cu-1% Pd/CeO_2 (UG) possessed a single broad peak similar to that shown in Fig. 8 (profile 'c'). Based on these observations, the sharp shoulders at 146 °C in DP catalyst (profile 'a') and at 132 °C in the IWI catalyst are assigned to the reduction of a part of Pd supported on CeO_2 and the main broad peak is attributed to the reduction of both Pd and CuO supported on CeO_2. Depending upon the method of Pd loading and the nature of Pd precursor used, the reduction of PdO has been observed in the temperature range between 130 and 260 °C [24]. In the case of CuO-supported CeO_2 catalyst, several research groups have observed at least two reduction regions, one below 175 °C and the other above 200 °C [20,26,30]. The peak below 175 °C has been generally assigned to the reduction of dispersed CuO clusters while the peak above 200 °C has been attributed to the reduction of CuO particles, similar to that of bulk CuO. As mentioned above, the catalyst without Pd exhibits three distinct peaks, two peaks below 200 °C and the third peak above 200 °C, indicating the formation of at least two different CuO clusters dispersed on the CeO_2 support together with some bulk-like CuO particles. However, the presence of Pd along with Cu makes the CuO reduction as a single broad peak. This suggests that in addition to the Pd–Ce and Cu–Ce interactions, as evidenced from the XPS studies (Figs. 6 and 7), a Cu–Pd interaction also exists in the catalyst. The synergistic interaction between Cu and Pd further improves the reducibility of Cu and Pd species. In fact, a recent in situ X-ray absorption near edge structure (XANES) study on the similar Cu-Pd/CeO_2-ZrO_2-Al_2O_3 catalyst confirmed the formation of Cu–Pd alloy and this significantly improved the catalytic performance of CO–O_2–NO reaction [29]. Thus, in addition to a lower copper surface concentration (higher copper metal dispersion) and better Cu–Ce and Pd–Ce interactions as observed from XPS studies, the better reducibility of Cu and Pd particles in the IWI catalyst could also contribute to the improved catalytic performance.

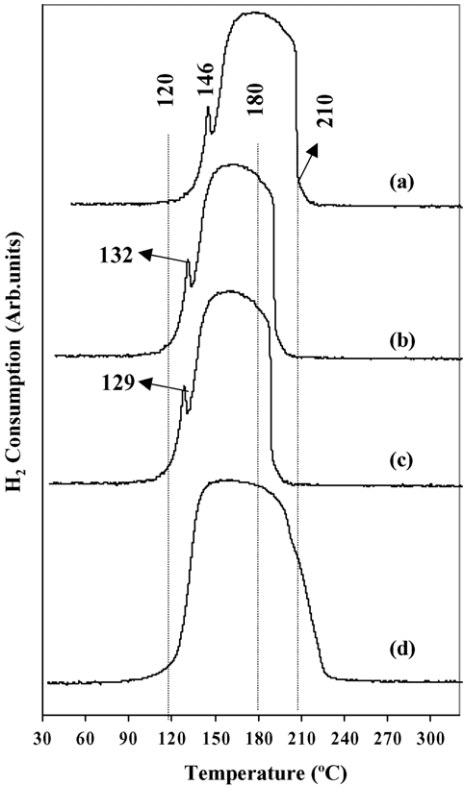

Fig. 8. TPR profiles of (a) DP Cu (30)-Pd (1)/CeO_2 (comm.), (b) IWI Cu (30)-Pd (1)/CeO_2 (comm.), (c) IWI Cu (30)-Pd (1)/CeO_2 (UG), (d) IWI Cu (30)-Pd (1)/CeO_2 (TA).

3.5. Effect of nature of CeO_2 support

In an effort to understand the effect of nature of CeO_2 support on the catalytic performance in the WGS reaction, the CeO_2 (comm.), CeO_2 (UG), and CeO_2 (TA) have been used as supports for 30 wt% Cu and 1 wt% Pd. Since the catalyst prepared by IWI method exhibited better catalytic performance, this method has been employed for the preparation of Cu-Pd bimetallic catalysts with three

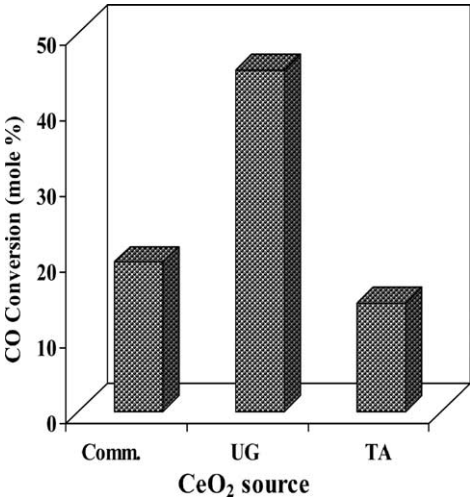

Fig. 9. Effect of the nature of CeO_2 support on the catalytic performance in the WGS reaction over Cu-Pd bimetallic catalyst containing 30% Cu and 1% Pd loaded by incipient wetness impregnation; feed compositions: 0.2% CO, 10% CO_2, 40.0% H_2O, and balance Ar.

different CeO_2 supports. The catalytic performance in the OWGS reaction over IWI Cu (30)-Pd (1)/CeO_2 (comm.), IWI Cu (30)-Pd (1)/CeO_2 (UG), and IWI Cu (30)-Pd (1)/CeO_2 (TA) catalysts is compared in Fig. 9 under a set of similar experimental condition. The CO conversion was kept below 50% in order to clearly recognize the difference in catalytic activity. It is clear from Fig. 9 that the Cu-Pd bimetallic catalyst supported on the CeO_2 prepared by urea gelation exhibits significantly higher CO conversion than the catalysts supported either on the CeO_2 (comm.) or CeO_2 (TA). The CO conversion decreases in the order CeO_2 (UG) > CeO_2 (comm.) > CeO_2 (TA). The observed trend has a direct correlation with BET surface area of the support (see Table 1). The BET surface area also decreases in the order: CeO_2 (UG) > CeO_2 (comm.) > CeO_2 (TA). Thus, the better catalytic performance of CeO_2 (UG) could be attributed to the higher BET surface area of the support that helps to achieve a higher metal dispersion.

The TPR profiles of Cu-Pd bimetallic catalysts supported on three different CeO_2 are included in Fig. 8 itself. As can be seen, there are significant differences in the position and shape of the peak. The position of the sharp shoulder and the peak maximum of the main peak are relatively lower in the catalyst with CeO_2 (UG) compared to the CeO_2 (comm.) (compare profiles 'b' and 'c'). The profile for CeO_2 (TA) is much broader and the completion of reduction occurs around 230 °C compared to below 200 °C for CeO_2 (comm.) and CeO_2 (UG) (compare profiles 'b', 'c', and 'd' in Fig. 8). Clearly, the catalyst with CeO_2 (TA) consists of large amount of bulk-like CuO that can be reduced only above 200 °C [20,26,30]. Thus, it is expected that this catalyst would consist of lower amount of dispersed CuO clusters that have good interaction with CeO_2 and are more active for OWGS reaction and as a consequence, exhibits poor performance compared to other CeO_2 analogues.

3.6. Effect of hydrogen co-feeding

The reformed gas obtained from alcohol or hydrocarbon reforming typically consists of 40–75% of H_2 along with 20–25% of CO_2 and 0.3–5% of CO. The presence of H_2, however, complicates the CO removal, especially in the preferential oxidation of CO (CO PrOx) to CO_2, because under the experimental conditions employed, H_2 also is oxidized and this decreases the overall efficiency of the fuel processor. Selective oxidation of CO in the reformed gas without oxidizing H_2 is a challenging task in producing fuel cell-grade H_2 gas. In order to investigate if the OWGS reaction over the Cu-Pd/CeO_2 catalysts developed in the present study retain the catalytic activity even under H_2-rich conditions, a simulated gas mixture containing 4% CO, 10% CO_2, and balance H_2 has been used as feed. The WGS and OWGS reactions have been performed under extremely high H_2 concentrations using CO/O_2 = 1/0.5 and CO/H_2O = 1/10. For comparison, the CO PrOx reaction has also been performed under similar experimental conditions and the data are shown in Fig. 10. Since the CeO_2 support synthesized by urea gelation exhibited the best performance (see Fig. 9), the catalyst, IWI Cu (30)-Pd (1)/CeO_2 (UG), has been employed for such a comparison. It is interesting to note that the OWGS reactions under the H_2-rich condition (H_2 + OWGS) exhibit a CO conversion very close to 100%. Under the same experimental conditions, the H_2 + WGS reaction without oxygen shows slightly lower CO conversion of around 95% while the CO PrOx reaction without added H_2O offers only about 65% CO conversion (see Fig. 10). These results reveal that the OWGS reaction is more selective for removing CO from the H_2-rich reformed gas compared to WGS or PrOx reactions over the present catalyst system. In fact, a comparison of data obtained from OWGS reaction using 2000 ppm CO and 4% CO in the feed

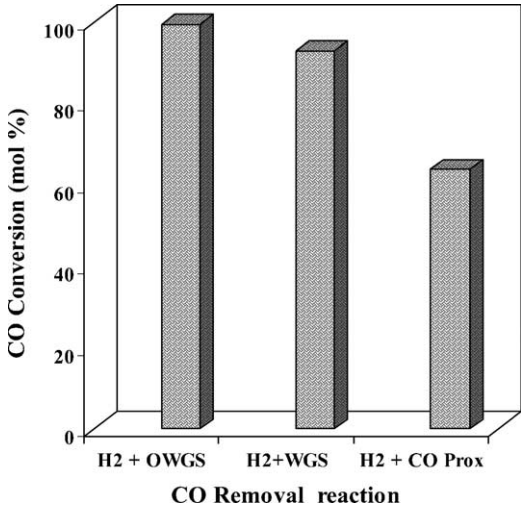

Fig. 10. Catalytic performance of IWI Cu (30)-Pd (1)/CeO_2 (UG) catalyst in the CO PrOx, WGS, and oxygen-assisted WGS reactions under extremely high H_2 concentration at 210 °C; feed compositions: 4% CO, 10% CO_2, CO/O_2 = 1/0.5 and CO/H_2O = 1/10, and balance H_2.

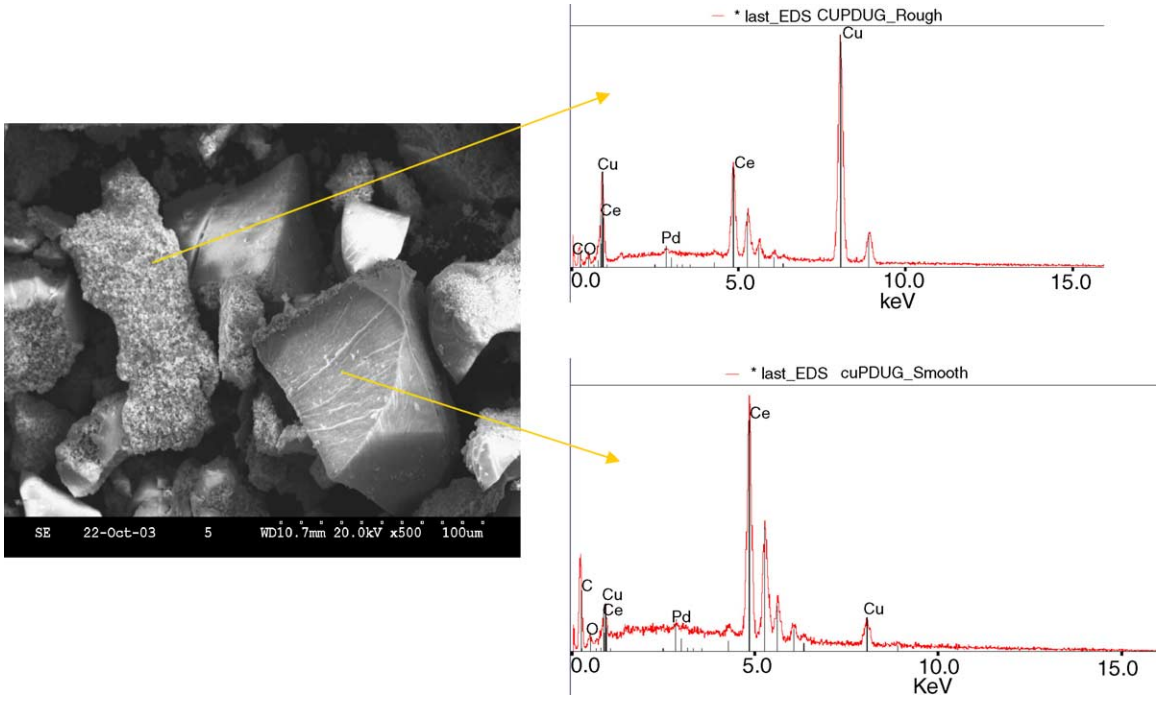

Fig. 11. SEM image (left) and EDX spectra (right) of fresh IWI Cu (30)-Pd (1)/CeO_2 (UG) catalyst.

gas revealed that the catalyst IWI Cu (30)-Pd (1)/CeO_2 (UG) performed better when 4% CO, $CO/O_2 = 1/0.5$ and $CO/H_2O = 1/10$ have been used in the feed rather than the initial conditions where 2000 ppm CO and a $CO/O_2 = 1/8$ has been employed. This is probably because the excess oxygen in the feed stream would preferentially oxidize hydrogen over CO. The low CO conversion achieved in the $H_2 + CO$ PrOx reaction could be due to the high reaction temperature of about 210 °C used under which the H_2 oxidation could strongly compete with CO oxidation.

3.7. Surface morphology of Cu-Pd/CeO_2 (UG)

The surface morphologies of Cu-Pd supported on CeO_2 (UG), the most active catalyst, has also been investigated by scanning electron microscopy (SEM) in order to understand the nature of Cu dispersion on CeO_2 support, and the image is displayed in Fig. 11. The image shows the existence of a mixture of smooth and rough surfaces of CuO and CeO_2 particles. The EDX spectra have also been recorded for the sample at two different spots and it is displayed along with the SEM image. The EDX analysis reveals that the rough surfaces consist of a large amount of CuO while the smooth surfaces are rich in CeO_2. These Cu-rich surfaces could be assigned to the bulk-like CuO particles, in view of immiscibility of CuO and CeO_2. Since Cu is lighter than Ce, smaller CuO clusters that are interacting closely with CeO_2 could not be detected by SEM. It is worth noting that similar Cu-rich and Ce-rich surfaces have also been observed in a co-precipitated and pre-reduced Cu/CeO_2 catalyst by transmission electron microscopy (TEM) [26]. However, at this stage, it is unclear if the rough CuO plays any significant role in catalytic activity of the present catalysts. Leaching of CuO in nitric acid to remove bulk-like CuO particles and evaluating the catalytic performance of leached Cu-Pd/CeO_2 catalyst would be very helpful to address this problem. Such experiments are currently in progress and will be reported in the near future.

4. Conclusions

Several conclusions could be drawn from the present study:

(i) Nano-crystalline CeO_2 with large BET surface area of about 215 m^2/g, higher than that of the commercially available high-surface-area CeO_2 source, has been synthesized using urea gelation technique.
(ii) Oxygen-assisted water–gas-shift reaction over Cu-Pd bimetallic catalysts supported on high-surface-area commercial CeO_2 indicated that Cu loading of about 30 wt% and Pd loadings of about 1 wt% exhibited a maximum CO conversion, close to 100%. No significant improvement in CO conversion has been observed between Cu loading of 2 and 20 wt% while a sharp rise in CO conversion has been observed with Cu loading above 20 wt%. Well-dispersed Cu clusters rather than highly dispersed Cu metals contribute to the CO conversion in the present catalyst system.
(iii) Method of Cu and Pd loadings plays significant role in catalytic performance. The catalyst prepared by

incipient wetness impregnation (IWI) exhibits higher CO conversion than the catalyst prepared by deposition–precipitation method. The IWI method leads to a lower Cu concentration and higher Ce concentration on the surface and consequently, a better Cu dispersion and Cu–Ce interaction could be achieved.

(iv) The synergistic interaction between Cu and Ce improves the reducibility of CuO. In addition to the Cu–Ce and Pd–Ce interactions, the catalysts also exhibit a strong Cu–Pd synergistic interaction, and that improves the reducibility of both Cu and Pd species.

(v) The catalytic activity for CO conversion seems to have a correlation with BET surface area of the CeO_2 support. The Cu-Pd bimetallic catalyst supported on high-surface-area CeO_2 obtained by urea gelation exhibits higher CO conversion than catalysts supported on commercial CeO_2 and those synthesized by template-assisted method.

(vi) The oxygen-assisted water–gas-shift reaction over a Cu-Pd bimetallic catalyst supported on a nano-sized CeO_2 synthesized by urea gelation exhibits CO conversion close to 100% even under extremely high H_2 concentration. The catalyst and the method developed in the present study are believed to be suitable for on-site or on-board purification of reformed gas for PEM fuel cell applications.

Acknowledgments

The authors are grateful to Conoco Phillips Petroleum Company and U.S. Department of Energy for supporting the first phase of our work on WGS using commercial Cu–ZnO catalysts in the Ultra Clean Fuels Project at Penn State under Instrument No. DE-FC26-01NT41098, which built the base for the current study to explore new catalysts for OWGS. We also wish to thank the Rhodia Chemical Company, USA, for the generous gift of high-surface-area CeO_2. Technical assistance from the Penn State Materials Characterization Lab for the XPS, MS-ICP, and SEM analysis is gratefully acknowledged.

References

[1] T.E. Springer, T. Rockward, T.A. Zawodzinski, S. Gottesfeld, J. Electrochem. Soc. 148 (2001) A11.
[2] J. Larminie, A. Dicks, Fuel Cell Systems Explained, John Wiley & Sons, New York, NY, 2000.
[3] C. Song, Catal. Today 77 (2002) 17.
[4] G. Sengupta, D.K. Gupta, S.P. Sen, Ind. J. Chem. 16A (1978) 1030.
[5] T. Utaka, K. Sekizawa, K. Eguchi, Appl. Catal. A: Gen. 194–195 (2000) 21.
[6] A. Ghenciu, Curr. Opin. Solid State Mater. Sci. 1 (2002) 389.
[7] K.M. Vanden Bussche, G.F. Froment, J. Catal. 161 (1996) 1.
[8] M. Sohrabi, A. Irandoukht, Afinidad 499 (2002) 267.
[9] R.A. Hadden, P.J. Lambert, C. Ranson, Appl. Catal. A: Gen. 122 (1995) L1.
[10] A. Prakash, Chem. Eng. Commun. 128 (1994) 143.
[11] K. Sekizawa, S. Yano, K. Eguchi, H. Arai, Appl. Catal. A: Gen. 169 (1998) 291.
[12] A. Worner, C. Friedrich, R. Tamme, Appl. Catal. A: Gen. 245 (2003) 1.
[13] L. Kundakovic, M. Flytzani-Slephanopoulos, J. Catal. 179 (1998) 203.
[14] Y. Zhang, S. Andersson, M. Muhammed, Appl. Catal. B: Environ. 6 (1995) 325.
[15] D.M. Lyons, K.M. Ryan, M.A. Morris, J. Mater. Chem. 12 (2002) 1207.
[16] Q. Fu, A. Weber, M. Flytzani-Stephanopoulos, Catal. Lett. 77 (2001) 87.
[17] Q. Fu, H. Saltsburg, M. Flytzani-Stephanopoulos, Science 301 (2003) 935.
[18] S. Velu, M.P. Kapoor, S. Inagaki, K. Suzuki, Appl. Catal. A: Gen. 245 (2003) 317.
[19] W. Gu, C. Song, Am. Chem. Soc. Fuel Chem. Div. Prepr. 48 (2003) 804.
[20] K. Li, Q. Fu, M. Flytzani-Slephanopoulos, Appl. Catal. B: Environ. 27 (2000) 179.
[21] D. Andreeva, V. Idakiev, T. Tabakova, L. Ilieva, P. Falaras, A. Bourlinos, A. Travlos, Catal. Today 72 (2002) 51.
[22] Y. Matsumura, W.-J. Shen, Top. Catal. 22 (2003) 271.
[23] W.-J. Shen, Y. Matsumura, Phys. Chem. Chem. Phys. 2 (2000) 1519.
[24] R. Gopinath, N. Lingaiah, B. Sreedhar, I. Suryanarayana, P.S.S. Prasad, A. Obuchi, Appl. Catal. B: Environ. 46 (2003) 587.
[25] S. Velu, K. Suzuki, C.S. Gopinath, H. Yoshida, T. Hattori, Phys. Chem. Chem. Phys. 4 (2002) 1990.
[26] Y. Liu, T. Hayakawa, T. Tsunoda, T. Suzuki, S. Hamakawa, K. Murata, R. Shiozaki, T. Ishii, M. Kumagai, Top. Catal. 22 (2003) 205.
[27] W. Liu, M. Flytzani-Stephanopoulos, J. Catal. 153 (1995) 304.
[28] W. Liu, M. Flytzani-Slephanopoulos, J. Catal. 153 (1995) 317.
[29] A.B. Hungria, A. Iglesias-Jez, A. Martinez-Arias, M. Fernandez-Garcia, J.A. Anderson, J.C. Conesca, J. Soria, J. Catal. 206 (2002) 281.
[30] P. Ratnasamy, D. Srinivas, C.V.V. Satyanarayana, P. Manikandan, R.S. Senthil Kumaran, M. Sachin, V.N. Shetti, J. Catal. 221 (2004) 455.
[31] S. Velu, K. Suzuki, C.S. Gopinath, J. Phys. Chem. B 106 (2002) 12737.
[32] K. Sekizawa, S.-I. Yano, K. Eguchi, H. Arai, Appl. Catal. A: Gen. 169 (1998) 291.
[33] Y. Matsumura, W.-J. Shen, Y. Ichihashi, M. Okumura, J. Catal. 197 (2001) 267.
[34] W.-J. Shen, Y. Ichihashi, H. Ando, M. Okumura, A. Haruta, Y. Matsumura, Appl. Catal. A: Gen. 217 (2001) 165.
[35] H.C. Yao, Y.F.Y. Yao, J. Catal. 86 (1984) 254.